Journal of Cellular Biochemistry 83:14–20 (2001)

Protein Tyrosine Phosphatase SHP-1 Specifically Recognizes C-Terminal Residues of Its Substrates Via Helix α0

Jian Yang,[1] Zhiliang Cheng,[1] Tianqi Niu,[1] Xiaoshan Liang,[1] Zhizhuang Joe Zhao,[2] and G. Wayne Zhou[1]*

[1]Program in Molecular Medicine, University of Massachusetts Medical School, Worcester, Massachusetts 01605

[2]Department of Medicine, Vanderbilt University, Nashville, Tennessee 37232

Abstract The catalytic domain of protein tyrosine phosphatase SHP-1 possesses distinct substrate specificity. It recognizes the P-3 to P-5 residues of its substrates via the β5-loop-β6 region. To study the substrate specificity further, we determined the structure of the catalytic domain of SHP-1 (C455S) complexed with a less-favorable-substrate peptide originated from SIRPα. The complex has disordered N-terminal peptide structure and reduced interactions between the N-terminal peptide and the β5-loop-β6 region. This could be the basis for the lower affinity of peptide pY^{427} for the catalytic domain of SHP-1. In addition, by comparing the SHP-1/less-favorable peptide complex structure with the SHP-1/substrate complex structures, we identified a novel substrate-recognition site in the catalytic domain of SHP-1. This site was formed by helix α0 and the α5-loop-α6 motif of SHP-1, and specifically bound residues at the P + 4 and further C-terminal positions of peptide substrates. J. Cell. Biochem. 83: 14–20, 2001. © 2001 Wiley-Liss, Inc.

Key words: protein tyrosine phosphatase; substrate specificity; phosphotyrosyl peptide; substrate-binding pocket

Protein tyrosine phosphatases (PTPs) are a group of enzymes that control cell growth, differentiation, and transformation through regulating the phosophorylation level of cellular proteins [Howard et al., 1994; Marengère et al., 1996; LaMontagne et al., 1998]. They can be broadly divided into receptor-like PTPs and cytosolic PTPs. The receptor-like PTPs are membrane bound and contain two tandem catalytic domains, whereas the cytosolic PTPs have only one copy of the catalytic domain. The catalytic domains of PTPs are highly conserved in their three-dimensional structures [Barford et al., 1994; Stuckey et al., 1994; Su et al., 1994; Yang et al., 1998]. However, they have remarkably different substrate specificity [Tenev et al., 1997; LaMontagne et al., 1998; O'Reilly and Neel, 1998; Tiganis et al., 1998]. The structural basis for the diverse substrate specificity of PTPs is still not understood. We have reported that the variable β5-loop-β6 motif confers PTP SHP-1 substrate specificity at the P-4 and further N-terminal subpockets [Yang et al., 2000]. In the present study, we continue to use SHP-1 and its physiological substrate SIRPα/SHPS-1 as a model to address the substrate specificity of PTPs.

PTP SHP-1 is expressed predominantly in hematopoietic cells, containing two *Src* homology 2 (SH2) domains, a neighboring catalytic domain, and an inhibitory C terminus. Domain-swapping studies on SHP-1 and its analogue, SHP-2, have shown that the catalytic domains of SHP-1 and SHP-2 have distinct substrate specificity [Tenev et al., 1997; O'Reilly and Neel, 1998], and therefore illustrate that dissecting the structural basis for the substrate specificity of SHP-1 is fundamental to understanding its physiological functions. The identification of the substrates of SHP-1, such as SIRPα, CD22, and

Jian Yang is a fellow of the H. Arthur Smith Foundation.

Grant sponsor: Career Development Award from the American Diabetes Association; Grant sponsor: Pilot project from DERC program of UMASS Medical School; Grant sponsor: NIH to GWZ; Grant number: AL45858; Grant sponsor: NIH to ZJZ; Grant number: HL57393.

*Correspondence to: G. Wayne Zhou, Program in Molecular Medicine, University of Massachusetts Medical School, 373 Plantation Street, Worcester, Massachusetts 01605.
E-mail: Wayne.Zhou@umassmed.edu

Received 26 February 2001; Accepted 13 April 2001

DOI 10.1002/jcb.1195

CD72 [Otipoby et al., 1996; Adachi et al., 1998; Timms et al., 1998], has made it possible for us to probe the structural basis.

SIRPα is a transmembrane protein of the signal-regulatory protein family. Its extracellular domain contains three immunoglobulin domains, and its cytoplasmic domain contains four phosphotyrosine sites pY^{427}, pY^{452}, pY^{469}, and pY^{495}. We synthesized four phosphotyrosyl decapeptides (from P−5 to P + 4 positions) with their sequences corresponding to the four tyrosine sites of SIRPα. For convenience, we also named the peptides after the phosphotyrosine sites. Kinetic studies of the catalytic domain of SHP-1 towards these four synthetic peptides have shown that peptide pY^{427} was not as good an in vitro substrate as peptides pY^{469} and pY^{495} [Yang et al., 2000]. However, peptide pY^{427} still exhibited lower K_m and much higher k_{cat}/K_m against the catalytic domain of SHP-1 compared to the kinetic parameters of the phosphotyrosyl peptides derived from epidermal growth factor receptor (EGFR) [Dechert et al., 1995]. To check the binding differences between the less-favorable peptide pY^{427} and the favorable in vitro peptide substrates pY^{469} and pY^{495} to the catalytic domain of SHP-1, and to examine the validity of other peptides, such as those derived from EGFR, for substrate specificity studies of SHP-1, we have determined the crystal structure of the catalytic domain of SHP-1 (C455S) complexed with peptide pY^{427}.

MATERIALS AND METHODS

Crystallization and Data Collection

The C455S mutant of the catalytic domain of SHP-1 (245-532) was cloned, expressed, and purified as described previously [Liang et al., 1997]. The enzyme was purified to better than 95% purity as judged by SDS electrophoresis gel, and concentrated to 5 mg/ml. Peptide pY^{427} (TNDITpYADLN) was synthesized and HPLC-purified to 90% purity by SynPep Inc. (Dublin, California). Crystals of the catalytic domain of SHP-1 were obtained by the vapor diffusion method with 4 μL protein drops (mixture of the protein solution and reservoir precipitating solution at 1:1 volume ratio), equilibrating over reservoir-precipitating solution (0.1 M Tris-HCl, pH 8.5, 1.9 M ammonium sulfate). The crystals were then soaked in the cryo-solvent (0.1 M Tris-HCl, pH 8.5, 1.9 M ammonium sulfate, 30% sucrose) containing 700 μM peptide pY^{427} for 2–3 days. A data set of the soaked complex was collected to 2.3 Å at −180°C on beamline F1 at CHESS (Cornell University). The data set was processed with Interactive DPS/Mosflm/CCP4 Data Processing software package [Szebenyl, 2000]. The crystal data is summarized in Table I.

Structure Determination

The complex structure of the catalytic domain of SHP-1 and peptide pY^{427} was solved by molecular replacement method using the program AMoRe [Navaza, 1994]. The coordinates of the catalytic domain of SHP-1 [Yang et al., 1998] were used as the initial search model. The molecular replacement solution was then refined using the rigid-body and positional protocols in the X-PLOR package [Brünger, 1992]. After five cycles of model re-building, a large piece of electron density was shown in the electron density difference map (F_o-F_c). Residue pTyr and residues at the C-terminal side of peptide pY^{427} were fit into the electron density. However, residues on the N-terminal side of residue pTyr of peptide pY^{427} were not observed even in the final electron density map. The model for the SHP-1-peptide pY^{427} complex was subjected to forty cycles of X-PLOR refinement, using the slowcool and positional refinement

TABLE I. Crystal Data and Refinement Results

Crystal data	
Unit cell	$a = 113.77$ Å, $b = 46.15$ Å, $c = 54.23$ Å
Space group	$P2_12_12$
Resolution (Å)	2.3
Data collection temperature (°C)	−180
R_{sym}	0.106
Data completeness (%)	91.3
Number of unique reflections	12008
Refinement	
R value	0.209
R-free	0.294
Resolution range (Å)	6.0-2.3
Number of reflections used in refinement	10242
Total number of protein non-H atoms	2242
Total number of peptide non-H atoms	46
Total number of water molecules	117
Estimated coordinate error (Å)	0.3
Average B-factor for enzyme non-H atoms (Å^2)	33.9
Average B-factor for peptide pY^{427} atoms (Å^2)	63.5
Average B-factor for water oxygen atoms (Å^2)	44.7
R.m.s. deviations for bond distances (Å)	0.008
R.m.s. deviations for bond distances (°)	1.46
R.m.s. deviations for dihedral angels (°)	25.2
R.m.s. deviations for impropers (°)	1.26

protocol [Brünger, 1992]. The refinement was carried out using the data better than 2σ and between 6 and 2.3 Å resolution. The model building interspersed with X-PLOR refinement was done by the program TURBO-FRODO [Roussel et al., 1990]. The *R-free* value was also calculated from the first to the penultimate cycle by randomly selecting 10% of the data as the test set. In addition, the occupancy for the observed residues of peptide pY^{427} was refined to 0.7. Multiple conformations for the β5-loop-β6 motif (residues 355–361) of SHP-1 were observed. However, only the closed conformation of the β5-loop-β6 motif showed clear, continuous electron density. The occupancy of the closed conformation for the β5-loop-β6 motif was also refined to 0.7. All other conformations of the β5-loop-β6 motif were not included in the model for latter refinement. In the final cycle of refinement, all reflections were used in the refinement. The final crystallographic *R-free* value and *R*-value were 0.294 and 0.209, respectively. The final model contains 2305 non-hydrogen atoms, including 117 water molecules. The final model shows good geometry as examined by using programs X-PLOR and PROCHECK [Laskowski et al., 1993]. The final refinement results are also summarized in Table I.

RESULTS AND DISCUSSION

Structural Determination

The SHP-1-peptide pY^{427} complex structure and the electron density map around peptide pY^{427} are shown in Figure 1. Unlike the SHP-1-peptide pY^{469} and SHP-1-peptide pY^{495} complex structures, only residues at the C-terminus to the phosphotyrosine of peptide pY^{427} were observed in the SHP-1/pY^{427} complex structure. The N-terminal residues of peptide pY^{427} were not observed due to inconclusive indication of their positions in the final electron density map. The occupancy of the observed residues of peptide pY^{427} was refined to 0.7. The average B-factor for these observed residues of peptide pY^{427} was 63.5 $Å^2$, higher than that of 33.9 $Å^2$ for the catalytic domain of SHP-1. This implicated that the observed phosphotyrosine and C-terminal residues of peptide pY^{427} were flexible and the binding of peptide pY^{427} to the catalytic domain of SHP-1 was weak. The low occupancy of peptide pY^{427} and weak interaction between the catalytic domain of SHP-1 and

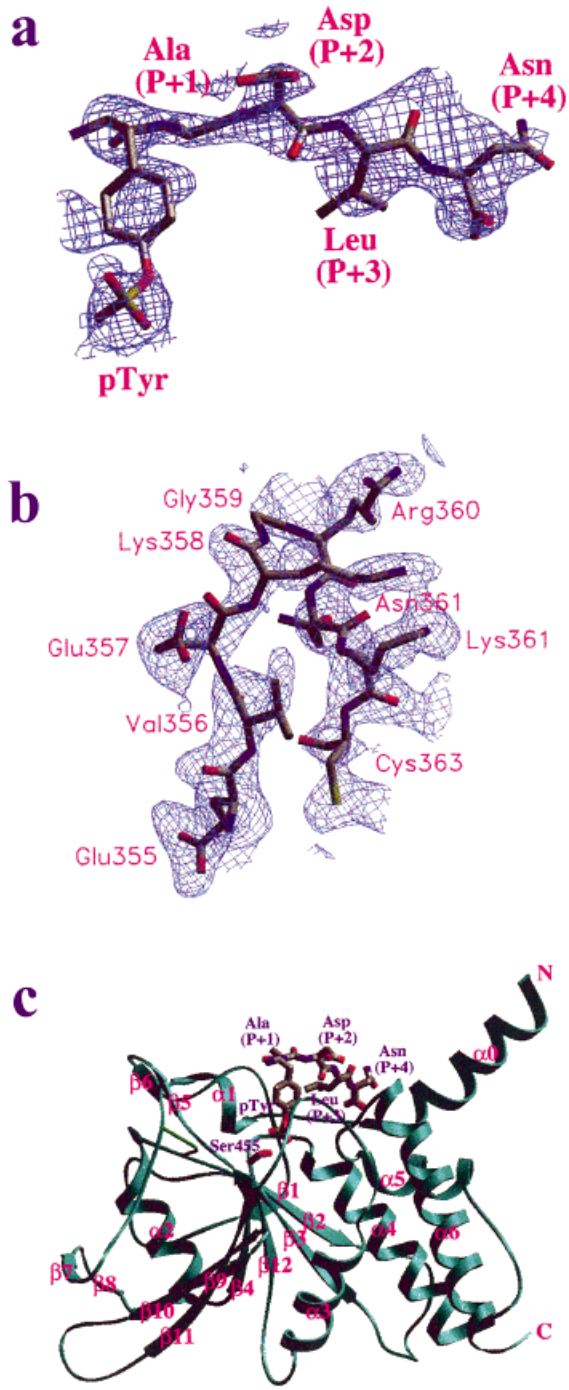

Fig. 1. **a:** The final electron density map ($2F_o-F_c$) contoured around the observed residues of peptide pY^{427}. The contour level of the map is 1σ, with the refined model of peptide pY^{427} shown in yellow. **b:** The final electron density map ($2F_o-F_c$) contoured around the β5-loop-β6 region. The contour level of the map is 1σ, with the refined model shown in yellow. The amino acids are labeled. **c:** A ribbon representation of the SHP-1-pY^{427} complex structure, with peptide pY^{427} shown in *stick* model and the catalytic domain of SHP-1 shown in green. These figures were prepared by SETOR [Evans, 1993].

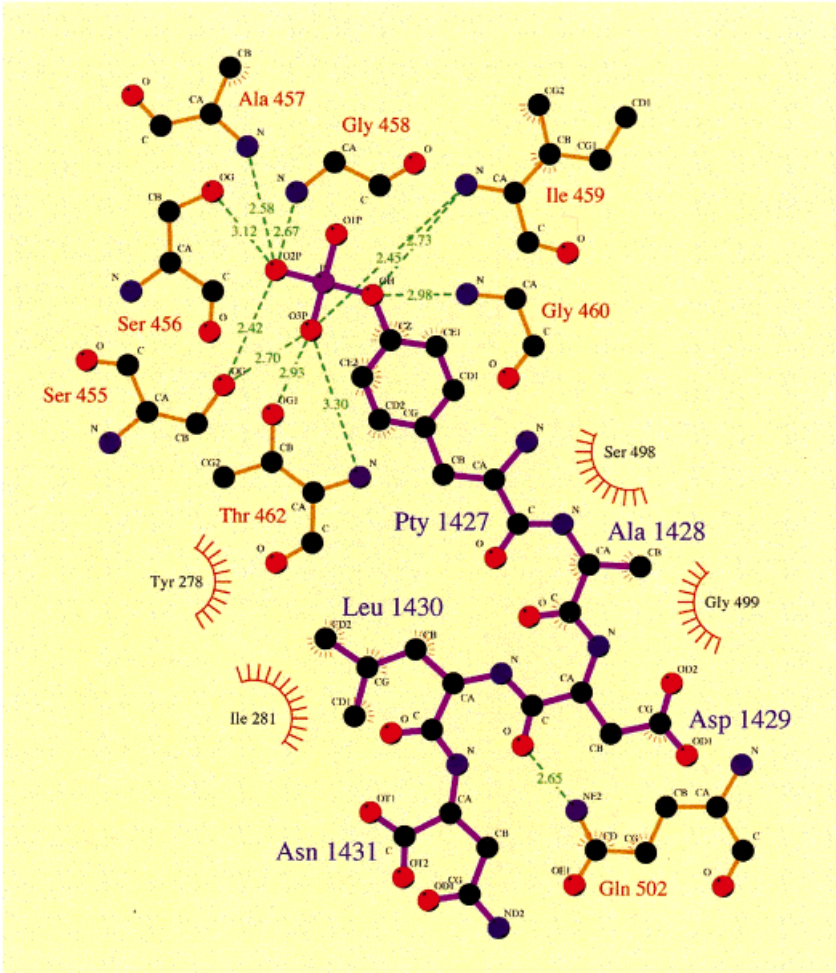

Fig. 2. A schematic representation of the interactions formed between the catalytic domain of SHP-1 and peptide pY^{427}. The figures were prepared by LIGPLOT [Wallace et al., 1995].

peptide pY^{427} were caused by two factors. Firstly, peptide pY^{427} was not a good in vitro substrate of the catalytic domain of SHP-1 [Yang et al., 2000]. Secondly, the K_m of the catalytic domain of SHP-1 towards peptide pY^{427} was 312 μM. Therefore, the peptide concentration (700 μM) used in the crystal-soaking might not be high enough to make peptide pY^{427} fully occupy the crystals.

We previously reported that the β5-loop-β6 motif conferred SHP-1 substrate specificity at the P-4 and further N-terminal subpockets [Yang et al., 2000]. Upon binding the peptide substrates, the β5-loop-β6 motif of SHP-1 underwent a 6-6.5 Å movement towards the substrates. However, in the SHP-1-pY^{427} complex, the β5-loop-β6 motif was present in multiple conformations. The closed conformation, as in the final model, was dominant, showing clear and continuous electron density with the occupancy refined to 0.7 (Fig. 1b). The consistency of occupancies between peptide pY^{427} and the closed conformation of the β5-loop-β6 motif implicated that the closed conformation of the β5-loop-β6 motif was induced by the binding of peptide pY^{427}. However, the β5-loop-β6 motif of SHP-1 did not have specific interactions with the N-terminal residues of peptide pY^{427}, which explained why peptide pY^{427} was not a good in vitro substrate of the catalytic domain of SHP-1.

Substrate Binding Sub-Pockets

The catalytic domain of SHP-1 interacts with peptide pY427 via both hydrogen bonds and van der Waals contacts. Schematic representations of those interactions are shown in Figure 2. The substrate-binding subpockets for the observed residues of peptide pY^{427} were well defined.

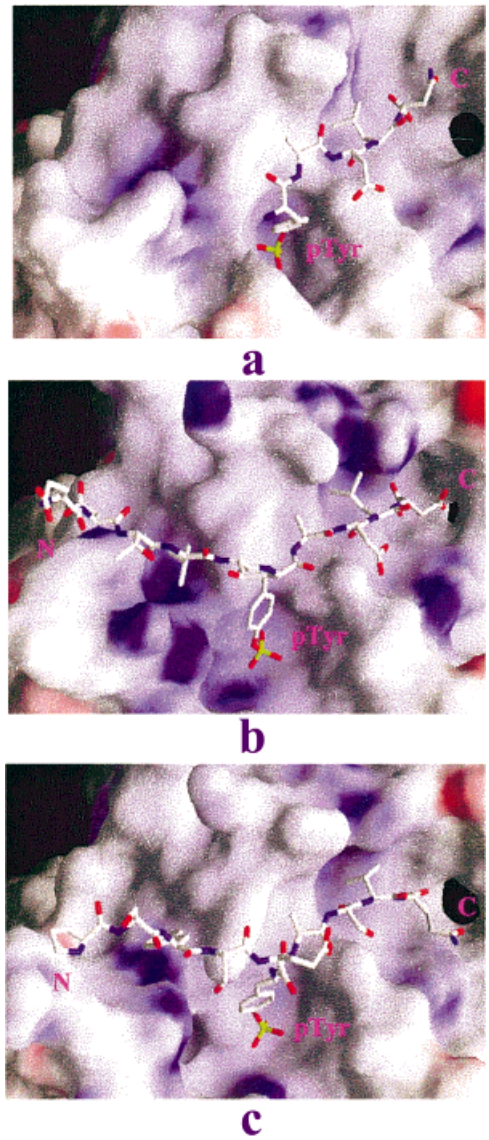

Fig. 3. Surface comparison of the SHP-1-pY^{427} (**a**) complex with the SHP-1-pY^{469} (**b**), and SHP-1-pY^{495} (**c**) complexes. The three complexes were superimposed on the catalytic domain of SHP-1. The catalytic domain of SHP-1 was shown in the *surface electrostatic potential* model, with red and blue representing negative and positive electrostatic potentials, respectively. The peptides were shown in the stick model. This figure was prepared by GRASP [Nicholls et al., 1991].

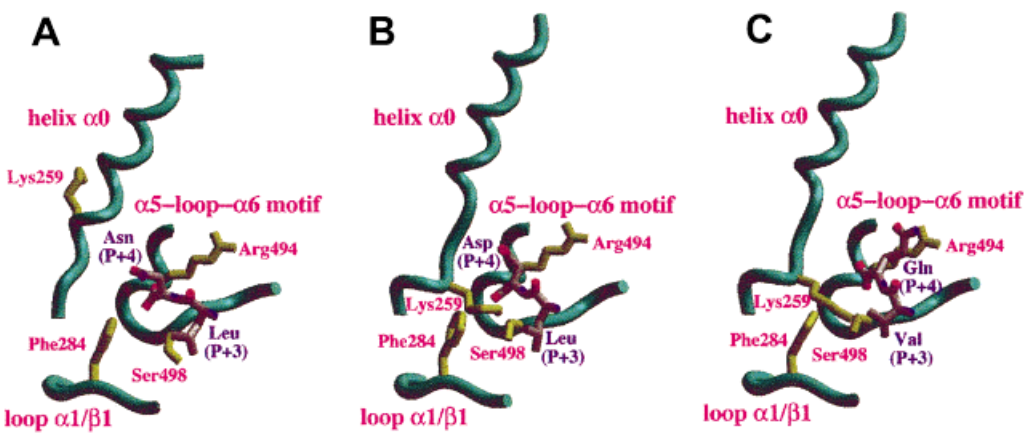

Fig. 4. Comparison of the P + 4 binding pocket among three different SHP-1-peptide complexes: (**A**) SHP-1-pY^{427} complex, (**B**) SHP-1-pY^{469} complex, and (**C**) SHP-1-pY^{495} complex. The P + 4 binding pocket was formed by three regions: helix α0, loop α1/β1, and α5-loop-α6 motif. The backbone of these three regions is shown in green, and the side chains of the amino acids interacting with the peptide substrates are shown in yellow. The amino acids at the P + 3 and P + 4 positions of the peptide are shown in *stick* model.

The pTyr-binding subpocket of the catalytic domain of SHP-1 was situated at a deep cleft on the surface of the molecule. The base of the subpocket was formed by the PTP signature motif HCXAGXGRS/T. The PTP signature motif formed a network of hydrogen bonds with the phosphate group of residue pTyr (Fig. 2). The hydroxyl oxygen atom of the mutated residue Ser^{455} was 3.0 Å from the phosphorus atom of residue pTyr. The hydrophobic walls of the pTyr subpocket were formed mainly by residues Tyr^{278}, Ile^{281}, His^{422}, and Gln^{502}. The $\pi-\pi$ interactions formed between residue Tyr^{278} of the catalytic domain of SHP-1 and residue pTyr of peptide pY^{427} were not as good as those observed in the complex formed between the catalytic domain of SHP-1 and peptide pY^{469}. This implicated that peptide pY^{427} was not a good in vitro substrate of the catalytic domain of SHP-1 as peptide pY^{469} and peptide pY^{495}.

The P + 1 subpocket was formed exclusively by residues Tyr^{278}, Ile^{281}, and Asn^{280} from loop $\alpha1/\beta1$. It was a large hydrophobic subpocket. However, the residue that occupied this subpocket was an alanine. Therefore, larger residues like valine, leucine, or isoleucine may be able to fit into this subpocket. The P + 2 subpocket was formed mainly by residue Gln^{502} of the catalytic domain of SHP-1. Residue Asp^{P+2} of peptide pY^{427} formed two hydrogen bonds with side chain N_ε atom of Gln^{502} through its main chain carbonyl oxygen atom and side chain carboxyl oxygen atom with distances at 2.65 and 2.74 Å, respectively. Since Gln^{502} is highly conserved in PTPs [Yang et al., 2000], residues such as serine, threonin, aspartate, asparagine, glutamate, and glutamine that may form hydrogen bonds with Gln^{502}, might be preferred for the P + 2 position of phosphotyrosyl peptides. The P + 3 subpocket was hydrophobic and formed by residues Ser^{498}, Asn^{280}, Ile^{281}, and Arg^{264} of the catalytic domain of SHP-1. Two weak hydrogen bonds were formed between the carbonyl oxygen atom of Asn^{280} and the side chain guanidine group of Arg^{264}. The P + 4 subpocket was mainly formed by residue Phe^{284} from loop $\alpha1/\beta1$ and residues Arg^{494}, Ser^{498}, and Gly^{499} from the $\alpha5$-loop-$\alpha6$ motif of the catalytic domain of SHP-1. The binding of Asn^{P+4} of peptide pY^{427} to the P + 4 subpocket was very loose. Asn^{P+4} was more exposed to the solvent than any other residues in decapeptide pY^{427}.

Novel Substrate-Recognition Site

Since peptide pY^{427} was a much less favorable in vitro substrate than Peptides pY^{469} and pY^{495}, we compared the structure of the SHP-1-pY^{427} complex with the structures of the SHP-1-pY^{469} and SHP-1-pY^{495} complexes in order to examine their binding differences (Fig. 3). With respect to peptide pY^{469}, residue pTyr of peptide pY^{427} shifted slightly towards the C-terminal side in the SHP-1-pY^{427} complex (Fig. 3a). The shift of residue pTyr was probably due to the weak binding of SHP-1 towards peptide pY^{427} and the disordered N-terminal residues.

The significant binding difference was observed at the P + 4 subpocket between the SHP-1-pY^{427} complex and the SHP-1-pY^{469} and SHP-1-pY^{495} complexes (Fig. 4). Compared to peptides pY^{469} and pY^{495} in the SHP-1-peptide complexes, residue Asn^{P+4} of peptide pY^{427} in the SHP-1-pY^{427} complex was more exposed to solvent. Residue Asn^{P+4} interacted only with residue Phe^{284} from loop $\alpha1/\beta1$ and residues Arg^{494}, Ser^{498}, and Gly^{499}, from the $\alpha5$-loop-$\alpha6$ motif. Residue Asn^{P+4} of peptide pY^{427} did not make any contacts with helix $\alpha0$. However, in the SHP-1-pY^{469} and SHP-1-pY^{495} complexes, residue Lys^{259}, which was located in helix $\alpha0$, rotated about 180°, disrupted the last helical turn of helix $\alpha0$ (residues 256–259), and interacted with the P + 4 residue (Asp^{P+4} in peptide pY^{469}, Fig. 3b, Gln^{P+4} in peptide pY^{495}, Fig. 3c). In this case, the P + 4 subpocket in the SHP-1-pY^{469} and SHP-1-pY^{495} complexes was formed by residues from both the $\alpha5$-loop-$\alpha6$ motif and helix $\alpha0$. Residues 256–259 in the full-length SHP-1 structure and the corresponding residues in the full-length SHP-2 structure [Hof et al., 1998] were both in the α-helical conformation. Thus, the conformational change of the last helical turn of helix $\alpha0$ was induced by substrate binding in the SHP-1-pY^{469} and SHP-1-pY^{495} complexes. The present observation confirmed and supported that P + 4 and further C-terminal positions composed a second specific recognition region, in addition to the substrate-recognition site formed by the $\beta5$-loop-$\beta6$ motif of SHP-1 of the catalytic domain of SHP-1, as we indicated in our previous studies [Yang et al., 2000]. This second substrate-recognition site was formed by both the $\alpha5$-loop-$\alpha6$ motif and helix $\alpha0$, and interacted specifically with the P + 4 and further C-terminal residues of phosphotyrosyl peptides.

This accumulated data shows that the less-favorable-substrate peptide pY^{427} did bind to the catalytic domain of SHP-1. However, the N-terminal residues of peptide pY^{427} were disordered. The interactions between the N-terminal residues of peptide and β5-loop-β6 motif are reduced. We also identified that helix α0 and the α5-loop-α6 motif of SHP-1 formed a second substrate-recognition site that interacted with the C-terminal residues of peptide substrates, in addition to the substrate-recognition site, formed between the β5-loop-β6 motif and the N-terminal residues of peptides.

REFERENCES

Adachi T, Flaswinkel H, Yakura H, Reth M, Tsubata T. 1998. The B cell surface protein CD72 recruits the tyrosine phosphatase SHP-1 upon tyrosine phosphorylation. J Immunol 160:4662–4665.

Barford D, Flint AJ, Tonks NK. 1994. Crystal structure of human protein tyrosine phosphatase 1B. Science 263: 1397–1404.

Brünger AT. 1992. X-PLOR Manual, Version 3.1. New Haven, Connecticut: Yale University.

Dechert U, Affolter M, Harder KW, Matthews J, Owen P, Clark-Lewis I, Thomas ML, Aebersold R, Jirik FR. 1995. Comparison of the specificity of bacterially expressed cytoplasmic protein-tyrosine phosphatases SHP and SH-PTP2 towards synthetic phosphopeptide Substrates. Eur J Biochem 231:673–681.

Evans SV. 1993. SETOR: hardware-lighted three-dimensional solid model representations of macromolecules. J Mol Graph 11:134–138.

Hof P, Pluskey S, Dhe-Paganon S, Eck MJ, Shoelson SE. 1998. Crystal structure of the tyrosine phosphatase SHP-2. Cell 92:441–450.

Howard PK, Gamper M, Hunter T, Firtel RA. 1994. Regulation by protein-tyrosine phosphatase PTP2 is distinct from that by PTP1 during Dictyostelium growth and development. Mol Cell Biol 14:5154–5164.

LaMontagne KR Jr, Hannon G, Tonks NK. 1998. Protein tyrosine phosphatase PTP1B suppresses p210 bcr-abl-induced transformation of rat-1 fibroblasts and promotes differentiation of K562 cells. Proc Natl Acad Sci USA 95:14094–14099.

Laskowski RA, MacArthur MW, Hutchinson SG, Thornton JM. 1993. PROCHECK: a program to check the stereochemical quality of protein structures. J Appl Crystallogr 26:283–291.

Liang X, Meng W, Niu T, Zhao Z, Zhou GW. 1997. Expression, purification, and crystallization of the catalytic domain of protein tyrosine phosphatase SHP-1. J Struct Biol 120:201–203.

Marengère LE, Waterhouse P, Duncan GS, Mittrücker HW, Feng GS, Mak TK. 1996. Regulation of T cell receptor signaling by tyrosine phosphatase SYP association with CTLA-4. Science 272:1170–1173.

Navaza J. 1994. AMoRe: an automated package for molecular replacement. Acta Crystallogr Sect A 50:157–163.

Nicholls A, Sharp K, Honig B. 1991. Protein folding and association: insights from the interfacial and thermodynamic properties of hydrocarbons. Proteins 11:281–296.

Otipoby KL, Andersson KB, Draves KE, Klaus SJ, Farr AG, Kerner JD, Perlmutter RM, Law CL, Clark EA. 1996. CD22 regulates thymus-independent responses and the lifespan of B cells. Nature 384:634–637.

O'Reilly AM, Neel BG. 1998. Activated mutants of SHP-2 preferentially induce elongation of Xenopus animal caps. Mol Cell Biol 18:161–177.

Roussel A, Foutecilla-Camps JC, Cambillau C. 1990. TURBO-FRODO: a new program for protein crystallography and modelling. Acta Crystallogr Sect A 46:C66.

Stuckey JA, Schubert HL, Fauman EB, Zhang ZY, Dixon JE, Saper MA. 1994. Crystal structure of Yersinia protein tyrosine phosphatase at 2.5 A and the complex with tungstate. Nature 370:571–575.

Su XD, Taddei N, Stefani M, Ramponi G, Nordlund P. 1994. The crystal structure of a low-molecular-weight phosphotyrosine protein phosphatase. Nature 370 575–578.

Szebenyl M. 2000. Interactive DPS/Mosflm/CCP4 Data Processing, Version 1.33, Ithaca, New York: Cornell University.

Tenev T, Keilhack H, Tomic S, Stoyanov B, Stein-Gerlach M, Lammers R, Krivtsov AV, Ullrich A, Böhmer FD. 1997. Both SH2 domains are involved in interaction of SHP-1 with the epidermal growth factor receptor but cannot confer receptor-directed activity to SHP-1/SHP-2 chimera. J Biol Chem 272:5966–5973.

Tiganis T, Bennett AM, Ravichandran KS, Tonks NK. 1998. Epidermal growth factor receptor and the adaptor protein p52Shc are specific substrates of T-cell protein tyrosine phosphatase. Mol Cell Biol 18:1622–1634.

Timms JF, Carlberg K, Gu H, Chen H, Kamatkar S, Nadler MJS, Rohrschneider LR, Neel BG. 1998. Identification of major binding proteins and substrates for the SH2-containing protein tyrosine phosphatase SHP-1 in macrophages. Mol Cell Biol 18:3838–3850.

Wallace AC, Laskowski RA, Thornton JM. 1995. LIGPLOT: a program to generate schematic diagrams of protein-ligand interactions. Prot Eng 8:127–134.

Yang J, Liang X, Niu T, Meng W, Zhao Z, Zhou GW. 1998. Crystal structure of the catalytic domain of protein-tyrosine phosphatase SHP-1. J Biol Chem 273:28199–28207.

Yang J, Cheng Z, Niu T, Liang X, Zhao ZJ, Zhou GW. 2000. Structural basis for substrate specificity of protein-tyrosine phosphatase SHP-1. J Biol Chem 275:4066–4071.